2016 International Symposium on Nonlinear Theory and Its Applications,
NOLTA2016, Yugawara, Japan, November 27th-30th, 2016

Discordant Alternans and Codimension-three Bifurcations in Coupled Luo-Rudy Models

Hiroyuki Kitajima and Toru Yazawa

†Faculty of Engineering, Kagawa University
2217–20 Hayashi, Takamatsu, Kagawa 761-0396, Japan
Email: kitaji@eng.kagawa-u.ac.jp, tyazawa@eng.kagawa-u.ac.jp

Abstract—Electrical alternans is the alternating amplitude from beat to beat in the action potential of the cardiac cell. Spatial pattern of the alternans in the heart is classified into two types: concordant and discordant alternans. The former and latter indicate spatially uniform and nonuniform distribution of the alternans. In this study, we investigate bifurcations for a system of coupled two Luo-Rudy models. As a result, we clarify the bifurcational mechanism of generating discordant alternans. Moreover, we determine existence of codimension-three bifurcations related to generation of discordant alternans.

1. Introduction

Electrical alternans is a beat to beat alternation in the action potential duration or amplitude of the cardiac cell [1, 2, 3, 4, 5, 6, 7, 8, 9, 10, 11, 12, 13]. Alternans is classified into eight or more kinds in [2]. Occurrence of the voltage or calcium-driven cellular alternans is explained by using action potential duration (APD) restitution, calcium dynamics, or voltage-calcium coupling, which is the dynamics in cellular level. On the other hand, the concordant and discordant alternans occur in tissue level. The former and latter corresponds to an in-phase and anti-phase synchronized solution in a system of coupled cells. The discordant alternans is related to QRS alternans and triggers wave break and ventricular fibrillation (VF) [2, 14, 15, 16, 17, 18, 19]. The generation mechanism of the discordant alternans is usually explained by interaction of APD and conduction velocity. However, the studies of the discordant alternans from the viewpoint of the dynamical system is not clear as far as we know.

In this paper, we study a system of coupled two Luo-Rudy I (LR) neurons [20] with synaptic inputs. We assume that the signals from the pacemaker cell are normal. We investigate the generation mechanism of the discordant alternans in the system. In a previous study [21], we clarified that alternans is generated by the period-doubling bifurcation due to changing the value of free concentration of the potassium ions in the extracellular compartment for the single LR model. In general, considering a system of coupled cells which have a period-doubling bifurcation, two types of the period-doubling bifurcation: symmetry-preserving and symmetry-breaking appear [22, 23, 24, 25, 26]. Moreover, the intersection of the two period-doubling bifurcations occurs in a parameter plane, which is referred as a codimension-three bifurcation, and the pitchfork bifurcations of a higher periodic solution appear [27].

Using the numerical bifurcation analysis method [28], we determined that the symmetry-preserving and symmetry-breaking period-doubling bifurcations generate the concordant and discordant alternans, respectively. Moreover, we found the parameter region of coexistence of two kinds of alternans. Biexcitability was reported [29, 30, 31], but these are for wave propagation in a two-dimensionally coupled system. In this study, we showed that the biexcitability is observed in a simpler system. We consider that the study of a small number of coupled cells is prototype to study the whole network because some groups composed of synchronized cells can be treated as one cell.

2. Preliminaries

3. System Equations

We use the LR model [20] for the sake of simplicity. The period of the external force (usually called “BCL”: basic cycle length) is assumed to be 380 [ms]. The membrane potentials V_1 and V_2 of coupled two LR models with the synaptic external input is described by

$$C\frac{dV_1}{dt} = -(I_1 + I_{syn} + G_v(V_1 - V_2)), \quad (1)$$

$$C\frac{dV_2}{dt} = -(I_2 + I_{syn} + G_v(V_2 - V_1)), \quad (2)$$

and the type and the dynamics for ionic currents I_i are given in Appendix. The synaptic current I_{syn} from the large cell to the muscle cell is given by

$$I_{syn} = G_{syn}(V - V_{syn})s(t^*), \quad (3)$$

where G_{syn} is the maximum synaptic conductance, V_{syn} is the reversal potential, and $s(t^*)$ is given by

$$s(t^*) = \frac{\tau_1}{\tau_2 - \tau_1}\left(-\exp\left(-\frac{t^*}{\tau_1}\right) + \exp\left(-\frac{t^*}{\tau_2}\right)\right), \quad (4)$$

where τ_1 and τ_2 are the raise and decay time of the synapse. We identify these values ($\tau_1 = 5.5$ and $\tau_2 = 90.0$[ms]) from the experimental data [32]. t^* is the time that is reset at every nT (n is a natural number, and T is the BCL). We check the periodicity of the trajectory by using the state variables at every nT. The values of the parameters related with the synapse are fixed as $G_{syn} = 4.0$ and $V_{syn} = -29.0$.

3.1. Symmetry

We assume that a system equation is described by

$$\frac{dx}{dt} = f(x), \quad x \in R^n \tag{5}$$

A system is called invariant with respect to g of a group G (or G-equivariant) if

$$gf(x) = f(gx), \forall g \in G. \tag{6}$$

The fixed-point subspace $X^G \subset R^n$ is defined as

$$X^G = \{x \in R^n : gx = x, \forall g \in G\}. \tag{7}$$

The set X^G is a linear subspace of R^n. This subspace is an invariant set of Eq. (5) [26, 33].

Considering our system ($n = 16$), the group G is formed by

$$G = \{g\}, \quad g = \left[\begin{array}{c|c} O & I_8 \\ \hline I_8 & 0 \end{array}\right] \tag{8}$$

where O and I_8 is zero and identity matrix, respectively. The fixed-point subspace X^G is given by

$$X^G = \{x \in R^{16} : gx = x\}. \tag{9}$$

We introduce the definitions of symmetric periodic solutions [26].

Definition 3.1 *A periodic solution $\psi(t)$ is called in-phase if $g\psi(t) = \psi(t)$ for all $t \in R$.*

Definition 3.2 *A periodic solution $\psi(t)$ with (minimal) period T_S is called anti-phase if*

$$g\psi(t) = \psi(t + T_S/2)$$

for all $t \in R$.

4. Results

We show a bifurcation diagram in Fig. 1. The negative value of G_v is no meaning in physiological sense, however, it is important from the viewpoint of the dynamical system because of existence of the intersection of double period-doubling bifurcations. Black thick lines denoted by I_1 and I_3 present symmetry-preserving period-doubling bifurcations, which means that an in-phase 2-periodic solution (Fig. 2(a)) is generated from an in-phase solution. Period-doubling bifurcation I_2 is symmetry-breaking which generates an anti-phase 2-periodic solution (Fig. 2(b)). The intersection points of these bifurcations (closed circles in Fig. 1) are called a codimension-three bifurcation. It is known that pitchfork bifurcations of 2-periodic solutions appear from these points, those are D_1^2 to D_3^2. We explain the detailed bifurcation structure around this codimension-three bifurcation point using Fig. 3.

Figure 3 is a schematic diagram along curve l in Fig. 1. At the starting point of l we observe stable in-phase 1-periodic solution which corresponds to a normal state in the cardiac system. Stable 2-periodic solutions synchronized at anti-phase are generated at ①. This solution (red curve in Fig. 3) meets pitchfork bifurcation D_2^2 and becomes unstable at ④. It disappears at ⑤. The unstable in-phase 1-periodic solution (black dashed line) also meets period-doubling bifurcation at ② and unstable 2-periodic solutions are generated. The stability turns to stable at ③ by pitchfork bifurcation D_1^2. Thus, stable in-phase and anti-phase 2-periodic solutions coexist between ③ and ④. This region is shown as overlapping of green and hatched pattern in Fig. 1.

Figure 4 shows the difference between solutions denoted by red and green curves in Fig. 3 using the plane (V_1, V_2). The diagonal line ($V_1 = V_2$) represents the invariant subspace X^G given by Eq. (9). The trajectory of anti-phase (Fig. 4(a)) is symmetry with respect to the operation g in Eq. (8). On the other hand, we obtain another solution by the operation g for the solution without symmetry (Fig. 4(b)).

5. Conclusion

We investigated a system of coupled Luo-Rudy models. We introduced symmetries for the system and its solutions. Using them, we clarified period-doubling bifurcations into two types: symmetry-preserving and breaking. The concordant and discordant alternans are generated by the symmetry-preserving and breaking period-doubling bifurcations, respectively. We determined the parameter region of coexistence of these two alternans.

Acknowledgments

This work was supported by JSPS KAKENHI Grant Number 15K00405. We thank Prof. T. Yoshinaga of Tokushima University for providing his powerful bifurcation analysis tools.

References

[1] D.S. Rosenbaum, L.E. Jackson, J.M. Smith, H. Garan, J.N. Ruskin and R.J. Cohen, Electrical alternans and vulnerability to ventricular Arrhythmias, N. Engl. J. Med., 330, 235–241, 1994.

[2] A. Garfinkel, Eight (or more) kinds of alternans, Journal of Electrocardiology, 40(6), S70–S74, 2007.

[3] L.D. Wilson and D.S. Rosenbaum, Mechanisms of arrythmogenic cardiac alternans, Europace, 9(suppl 6), vi77–vi82, 2007.

[4] D.E. Euler, Cardiac alternans: mechanisms and pathophysiological significance, Cardiovascular Research, 42(3), 583–590, 1999.

[5] J.M. Smith, E.A. Clancy, C.R. Valeri, J.N. Ruskin and R.J. Cohen, Electrical alternans and cardiac electrical instability, Circulation, 77(1), 110–121, 1988.

[6] T. Yazawa, H. Kitajima and A. Shimizu, A simulation study of alternans-arrhythmia based on physiology of invertebrate heart, Proc. WCECS, 604–609, 2013.

[7] J.B. Nolasco and R.W. Dahlen, A graphic method for the study of alternation in cardiac action potentials, J. Appl. Physiol., 25, 191–196, 1968.

[8] M.L. Koller, M.L. Riccio and R.F. Gilmour, Dynamic restitution of action potential duration during electrical alternans and ventricular fibrillation, Am. J. Physiol. Heart Circ. Physiol., 275, 1635–1642, 1998.

[9] B. Echebarria and A. Karma, Instability and spatiotemporal dynamics of alternans in paced cardiac tissue, Physical Review E, 88, 208101, 2002.

[10] P. Jørgensen, C. Schäfer, P.G. Guerra, M. Talajic, S. Nattel and L. Glass, A mathematical model of human atrioventricular nodal function incorporating concealed conduction, Bulletin of Mathematical Biology, 64(6), 1083–1099, 2002.

[11] J. Sun, F. Amellal, L. Glass and J. Billette, Alternans and period-doubling bifurcations in atrioventricular nodal conduction, Journal of Theoretical Biology, 173(1), 79–91, 1995.

[12] E.G. Tolkacheva, M.M. Romeo, M. Guerraty and D.J. Gauthier, Condition for alternans and its control in a two-dimensional mapping model of paced cardiac dynamics, Physical Review E, 69(3), 031904, 2004.

[13] E.G. Tolkacheva, M.M. Romeo and D.J. Gauthier, Control of cardiac alternans in a mapping model with memory, Physica D, 194(3), 385–391, 2004.

[14] Z. Qu, A. Garfinkel, P.S. Chen and J.N. Weiss, Mechanisms of discordant alternans and induction of reentry in simulated cardiac tissue, Circulation, 102(14), 1664–1670, 2000.

[15] D. Sato, Y. Shiferaw, A. Garfinkel, J.N. Weiss, Z. Qu and A. Karma, Spatially discordant alternans in cardiac tissue role of calcium cycling, Circulation Research, 99(5), 520–527, 2006.

[16] M.A. Watanabe, F.H. Fenton, S.J. Evans, H.M. Hastings and A. Karma, Mechanisms for Discordant Alternans, Journal of Cardiovascular Electrophysiology, 12(2), 196–206, 2001.

[17] J.M. Pastore, S.D. Girouard, K.R. Laurita, F.G. Akar and D.S. Rosenbaum, Mechanism linking T-wave alternans to the genesis of cardiac fibrillation, Circulation, 99(10), 1385–1394, 1999.

[18] H. Hayashi et al., Dynamic origin of spatially discordant alternans in cardiac tissue, Biophysical journal, 92(2), 448–460, 2007.

[19] J.M. Pastore, K.R. Laurita and D.S. Rosenbaum, Importance of spatiotemporal heterogeneity of cellular restitution in mechanism of arrhythmogenic discordant alternans, Heart Rhythm, 3(6), 711–719, 2006.

[20] C.H. Luo and Y. Rudy, A model of the ventricular cardiac action potential. Demoralization, repolarization, and their interaction, Circ. Res., 68, 1501–1526, 1991.

[21] H. Kitajima, E. Ioka and T. Yazawa, Generation mechanism of alternans in Luo-Rudy model, Int. J. Bifurcation and Chaos, 26(5), 1650075, 2016.

[22] S.Y. Kim and H. Kook, Period doubling in coupled maps, Phys. Rev. E, 48(2), 785–799, 1993.

[23] S.Y. Kim, Universality of period doubling in coupled maps, Phys. Rev. E, 49(2), 1745, 1994.

[24] S.Y. Kim, Bicritical behavior of period doublings in unidirectionally coupled maps, Phys. Rev. E, 59, 6585, 1999.

[25] S.Y. Kim and W. Lim, Bicritical scaling behavior in unidirectionally coupled oscillators, Phys. Rev. E, 63(3), 036223, 2001.

[26] S.P. Kuznetsov, A.P. Kuznetsov and I.R. Sataev, Multiparameter critical situations, universality and scaling in two-dimensional period-doubling maps, Journal of Statistical Physics, 121(5-6), 697–748, 2005.

[27] H. Kitajima, T. Yoshinaga and H. Kawakami, Codimension two bifurcation observed in a phase converter circuit. IEICE Trans. on Fundamentals of Electronics, Communications and Computer Sciences, 79(10), 1563–1567, 1996.

[28] H. Kawakami, Bifurcation of periodic responses in forced dynamic nonlinear circuits: computation of bifurcation values of the system parameters, IEEE Trans. Circuits & Systs., CAS-31(3), 248–260, 1984.

[29] M.G. Chang et al., Bi-stable wave propagation and early afterdepolarization-mediated cardiac arrhythmias, Heart rhythm, 9(1), 115-122, 2012.

[30] M.G. Chang, E. de Lange, G. Calmettes, A. Garfinkel, Z. Qu and J.N. Weiss, Pro-and antiarrhythmic effects of ATP-sensitive potassium current activation on reentry during early afterdepolarization-mediated arrhythmias, Heart Rhythm, 10(4), 575-582, 2013.

[31] N. Vandersickel, I.V. Kazbanov, A. Nuitermans, L.D. Weise, R. Pandit and A.V. Panfilov, A study of early afterdepolarizations in a model for human ventricular tissue, PloS one, 9(1), e84595, 2014.

[32] T. Yazawa, J.L. Wilkens, H.E.D.J. ter Keurs and M.J. Cavey, Structure and contractile properties of the ostial muscle (musculus orbicularis ostii) in the heart of the American lobster, J. Comp. Physiol. B, 169, 529–537, 1999.

[33] M. Golubitsky, I. Stewart and D.G. Schaeffer, Singularities and Groups in Bifurcation Theory II, Springer-Verlag, New York, 1988.

Appendix

Ionic currents I_1 and I_2 in Eqs. (1) and (2) consist of following currents:

$$
\begin{aligned}
I_{Na} &= G_{Na} m^3 h j (V - E_{Na}), \quad \text{(sodium current)},\\
I_{Si} &= G_{Si} d f (V - E_{Si}), \quad \text{(slow inward current)},\\
I_K &= G_K X X_i (V - E_K), G_K = 0.282\sqrt{[K]_o/5.4},\\
& \quad E_K = \frac{RT}{F}\ln\left(\frac{[K]_o + PR_{NaK}[Na]_o}{[K]_i + PR_{Nak}[Na]_i}\right),\\
& \quad\quad \text{(time-independent potassium current)},\\
I_{K1} &= G_{K1} K1_\infty (V - E_{K1}), G_{K1} = 0.6047\sqrt{[K]_o/5.4},\\
& \quad E_{K1} = \frac{RT}{F}\ln\left(\frac{[K]_o}{[K]_i}\right),\\
& \quad\quad \text{(time-independent potassium current)},\\
I_{Kp} &= 0.0183 Kp (V - E_{Kp}), \quad \text{(plateau potassium current)},\\
I_b &= 0.03921 (V + 59.87), \quad \text{(background current)}.
\end{aligned}
$$

Detailed explanation of these equations is written in [20].

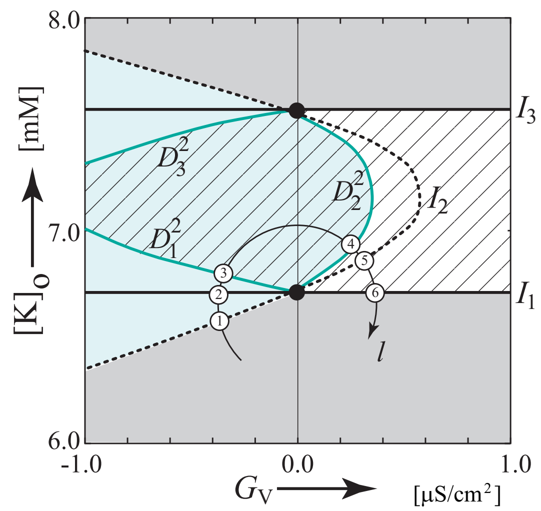

Figure 1: Bifurcation diagram for coupled LR models. Curves I and D indicate period-doubling and pitchfork bifurcations, respectively. We observe in-phase 1-periodic, anti-pahse 2-periodic, and in-phase 2-periodic solutions in gray, green, and hatched regions, respectively.

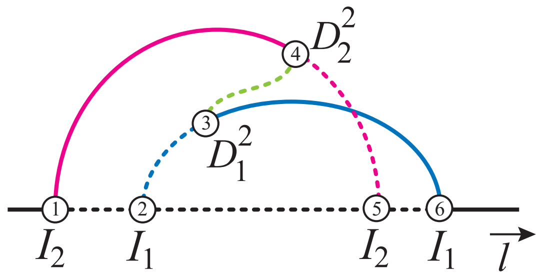

Figure 3: Schematic bifurcation diagram along curve l in Fig. 1. Solid and dashed curves indicate stable and unstable solutions, respectively. Black and blue curves represent in-phase solution. Red is used for anti-phase solution. Solution without symmetry are shown by green.

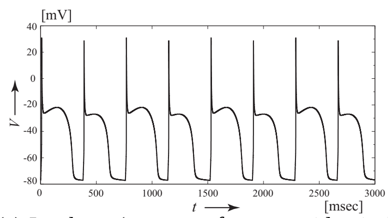

(a) In-phase (two waveforms are identical)

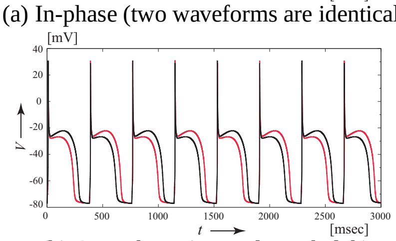

(b) Anti-phase (V_1: red, V_2: balck)

Figure 2: Waveforms of membrane potentials of two 2-periodic solutions at $G_V = 0.1$ and $[\mathrm{K}]_\mathrm{O}$=7.2

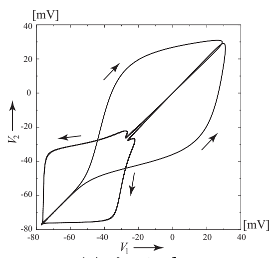

(a) Anti-phase

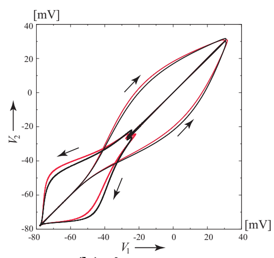

(b) Asymmetry

Figure 4: Trajectories in (V_1, V_2) plave for two 2-periodic solutinos. Arrows indicate the direction of trajectory. (a) one trajectory at $G_V = 0.1$ and $[\mathrm{K}]_\mathrm{O}$=7.2, (b) two trajectories denoted black and red at $G_V = 0.1$ and $[\mathrm{K}]_\mathrm{O}$=6.9.